Viscosity-sensitive emission of anionic hydrogen-bonded urea-derivative–acetate-ion complexes and their aggregation-induced emission enhancement

Masaki Takahashi (tmasaki@yamanashi.ac.jp)
University of Yamanashi https://orcid.org/0000-0001-6581-5241
Nozomu Ito
University of Yamanashi
Hayato Ninagawa
University of Yamanashi
Kohei Yazaki
University of Yamanashi
Yoshihisa Sei
Tokyo Institute of Technology
Makoto Obata
University of Yamanashi

Article

Keywords: Fluorescence, Ionic Hydrogen Bonding, Urea Groups, Aggregation-induced Emission Enhancement, Fluid Viscosity, Solid-state Emitting

Posted Date: November 14th, 2020

DOI: https://doi.org/10.21203/rs.3.rs-100706/v1

Version of Record: A version of this preprint was published at Communications Chemistry on December 2nd, 2021. See the published version at https://doi.org/10.1038/s42004-021-00601-3.

Abstract

Anions often quench fluorescence (FL). However, strong ionic hydrogen bonding between fluorescent dyes and anion molecules has the potential to control the electronic state of FL dyes, creating new functions via non-covalent interactions. Here, we propose a novel approach, utilising ionic hydrogen bonding between urea groups and anions, to control the electronic states of fluorophores and develop an aggregation-induced emission enhancement (AIEE) system. The AIEE ionic hydrogen-bonded complex (IHBC) formed between 1,8-diphenylnaphthalene (p-2urea), with aryl urea groups at the para-positions on the peri-phenyl rings, and acetate ions exhibits a remarkably high sensitivity to fluid viscosity compared with most conventional viscosity-sensitive dyes, and the FL quantum yield (QY) in ion-pair assemblies of the IHBC and tetrabutylammonium cations is more than five times higher than that of the IHBC in solution. Our versatile and simple approach for the design of AIEE dye facilitates the future development of viscosity probes and solid-state emitting materials.

Introduction

Light-emitting organic compounds have been known to emit only in dilute solution, with quenching occurring in the solid state due to intermolecular interactions[1]. However, in recent years, organic compounds that emit fluorescence (FL) in solid-state form but are quenched in dilute solution, called aggregation-induced emission (AIE) dyes, and those for which the emission quantum yield (QY) increases upon aggregation, aggregation-induced emission enhancement (AIEE) dyes, have been discovered[2, 3]. Recently, these compounds have been intensively studied by photochemists and materials scientists from the perspective of fundamental scientific interest and for their potential technological importance in applications such as light-emitting diodes[4], fluorogenic probes for explosive detection[5], monitoring environmental hazards[6], viscosity sensing[7], and bioimaging probes[8]. Typical strategies for the development of efficient solid-state light-emitting molecules include the introduction of a bulky substituents to prevent intermolecular interactions[9], the formation of *J*-aggregates[10, 11], the introduction of electron-donating or electron-withdrawing groups[4, 12-14], and the introduction of the molecular structures that exhibit excited-state intramolecular proton transfer[15, 16].

However, existing light-emitting efficiencies are not high, and there is a lack of diversity in the currently available molecular skeletons. Indeed, tetraphenyl ethane, the most typical AIE dye, having a simple structure, has a low FL QY of 15% in the solid state[17]. Therefore, the development of next-generation solid-state light-emitting organic materials by utilising non-covalent interactions has been attempted in recent years. Only a few successful demonstrations of solid-state emission induced by non-covalent interactions have been reported. These include a coordination bond between the p-orbital of borane compounds and the oxygen atom of aldehydes[18], acid–base interactions[19], isolation of fluorescent dyes by ionic lattices[20] and an anion–π^+ interaction[21]. The introduction of electron-donating and electron-withdrawing groups to π-conjugated molecular systems with rotatable covalent bonds is a strategy for AIEE dye synthesis.[4, 12, 13, 22] Molecules having the donor–π–acceptor (D–π–A) structure often show

viscosity-sensitive fluorescence and AIEE because of the suppression of a weakly emitting twisted intramolecular charge transfer (TICT) state, resulting in emission from a locally excited (LE) state or planar intramolecular charge transfer (PICT) state, in the solid state or in highly viscous solvents[23]. A contrasting strategy for controlling the electronic state of functional groups is to utilise non-covalent interactions. The addition of a Brønsted or Lewis acid to fluorescent dye with a Lewis basic functional group results in an increase in the electron-withdrawing character of the functional group[24, 25] and the addition of a molecular anion to a fluorescent dye with a urea or pyrrole group produces a strongly ionic hydrogen-bonded complex (IHBC), resulting in an increase in the electron-donating character of the functional group[26]. Even when the electronic state of the molecule is altered by these non-covalent interactions, the compounds can still potentially exhibit AIEE characteristics. In this study, we focused on the strong ionic hydrogen-bonding interaction between urea groups and anions and attempted to create novel non-covalent AIEE materials (Fig. 1).

Recently, fluorescent urea compounds have been studied to examine their interaction with anionic molecules. Because the FL colour changes of the urea compounds occur upon adding anions, these studies have mainly been conducted in solution-phase experiments. This behaviour has been characterised for the development of fluorescent molecular sensors for the detection of specific anionic molecules[26-29]. Moreover, the interaction between anions and fluorescent urea compounds in solution has been considered to be the cause of fluorescence quenching[30, 31], and the light-emission characteristics of fluorescent urea derivatives in the solid-state have almost never been examined[32]. We have developed a new molecular design for the two urea substituents at the ortho-positions on the peri-phenyl rings on the naphthalene ring (***p*-2urea**) based on the characteristics of the molecular structures of conventional AIEE dyes. Such dyes typically contain π-electron systems that connect two electron-donating groups, each of which are linked to the π-system via a rotatable single bond[8], or they include π-systems with sterically hindered phenyl groups (Fig. 1)[2]. In addition, the 1-phenyl naphthalene derivative ***p*-1urea**, having a less sterically hindered phenyl group, and ***m*-2urea,** a positional isomer of ***p*-2urea** in which the urea groups are less conjugated with naphthyl group, were also synthesised to investigate the emission characteristics affected by ionic hydrogen bonding between the urea groups and molecular anion and by ion-pair complexation with tetrabutylammonium cations.

Results And Discussion

The synthesis and characterisation of ***p*-1urea**, ***p*-2urea**, and ***m*-2urea** are described in the Supporting Information. In addition, single crystals of ***p*-2urea** were obtained by vapour diffusion of diethyl ether into a DMSO solution. Single-crystal X-ray diffraction analysis demonstrated that ***p*-2urea** forms a hydrogen-bonded solvate complex with DMSO. Oxygen atoms in DMSO interact with two NH groups in urea, forming bifurcated hydrogen bonds (Supplementary Fig. 5).

Combined density functional theory and time-dependent density functional theory (DFT/TD-DFT) calculations for the three compounds and the IHBC of the urea groups and anions were carried out. For the TD-DFT calculations, the geometries of the three urea derivatives without acetate anions were first optimised at the B3LYP/6-31G (d, p) level of theory. Then, using the optimised geometries, excitation energies were calculated at the CAM-B3LYP/6-31G+(d) level of theory[33, 34]. All calculations were performed by using the Gaussian 16 package[35] and a common practice with DFT calculations is to replace tert-butyl groups with methyl groups to simplify the calculations and decrease the computational time. The geometries of the IHBC were optimised before excitation energy calculations were carried out at the CAM-B3LYP/6-31G+(d) level of theory. The results of these calculations are shown in Supplementary Figure 8. ***p*-2Urea** and the IHBC of ***p*-2urea** and acetate are expected to possess different degrees of conjugation and different electronic structures. The computed highest occupied molecular orbital (HOMO) and lowest unoccupied molecular orbital (LUMO) of ***p*-2urea** without AcO^- were found to be delocalised over the entire π-system. In contrast, the computed HOMO of the ***p*-2urea**–acetate IHBC was localised on the phenyl urea group substituent of the naphthyl system, and the LUMO of the complex was localised on the naphthyl rings. In addition, the HOMO energy level of the IHBC is increased by the ionic hydrogen bonding between the urea groups and acetate anions. A red shift of the UV absorption spectrum was predicted by TD-DFT calculations due to the charge-transfer character of the anionic ***p*-2urea**–acetate complex (Supplementary Fig. 9 and Supplementary Table 2). Therefore, control of the electronic states of fluorescent molecules by non-covalent bonding and the realisation of AIEE characteristics and viscosity-sensitive fluorescence by switching between PICT and TICT fluorescence are expected for the IHBC.

Investigation of hydrogen bonding interactions by ^{1}H NMR and IR spectroscopies

In order to examine the ionic hydrogen bonding between the synthesised compound and acetate anions in solution and in the solid state, the evolution of the solution-phase ^{1}H NMR spectrum upon the addition of tetrabutylammonium acetate (TBAAc) was observed, and an IR spectrum of the solid-state complex was acquired.

First, the shifting of the ***p*-2urea** N–H proton peaks in the ^{1}H NMR spectrum was confirmed upon adding TBAAc to ***p*-2urea** in DMSO-d_6. The N–H proton peaks were shifted from approximately 8.3 ppm to approximately 11.3 ppm and became saturated (Supplementary Fig. 10). From these observations, it was deduced that the electron densities of the N–H protons in the urea group were reduced by the ionic hydrogen bonding with acetate in DMSO. It was previously established that urea compounds form strong ionic hydrogen bonds with acetate, even in highly polar solvents such as DMSO that are thought to inhibit weak hydrogen bonding[36].

In addition, FT-IR spectra were measured to confirm that the acetate and urea groups formed ionic hydrogen bonds, even in the solid state. As a result, the stretching vibration of the carbonyl of the urea

group was shifted from 1651 cm^{-1} to 1699 cm^{-1} upon the addition of 2 equiv of TBAAc (Supplementary Fig. 11). This result demonstrates that the urea groups of ***p*-2urea** form intermolecular hydrogen bonds, and the C=O bond in the urea group is weakened in the solid-state without TBAAc. In addition, ionic hydrogen bonding between the N–H protons of the urea groups and acetate ions occurs with the addition of TBAAc, and the weaker intermolecular hydrogen bonds between different urea groups are eliminated with the C=O bond in the urea groups becoming stronger[37]. From these results, it can be concluded that ***p*-2urea** forms an ionic hydrogen bond with acetate ions, both in DMSO and in the solid state.

Investigation of changes in the UV–visible absorption and fluorescence spectra upon the addition of TBAAc in solution

Changes in the ultraviolet–visible (UV–Vis) absorption spectrum of ***p*-2urea** in DMSO (150 μM) upon addition of TBAAc were investigated. The UV–Vis spectrum of ***p*-2urea** in DMSO shows maxima at 270 and 340 nm. Upon addition of up to 250 equiv of TBAAc, a red shift in the absorption of ***p*-2urea** and isosbestic points at 280 and 310 nm were observed (Fig. 2 a). The red shift may be attributed to an increase in energy of the HOMO due to the ionic hydrogen bonding between ***p*-2urea** and acetate ions. Upon further addition of excess TBAAc, an increase in the absorbance of ***p*-2urea** over a wide wavelength range was observed, and the isosbestic points were lost. The absorption changes were presumed to be caused by changes in the properties of the solution caused by the addition of excess amounts of TBAAc.

In contrast, the UV–Vis spectrum of ***m*-2urea** in DMSO includes a single maxima, at 264 nm. Upon addition of TBAAc (up to 250 equiv), the red shift of the longer absorption region that was seen for ***p*-2urea** was not observed, and only one isosbestic point, at 270 nm, was apparent (Fig. 2 b).

The molecular-orbital calculation results support the hypothesis that the difference in the change in absorption wavelength between the positional isomers depends on the ease of charge transfer along the long-axis direction of the molecule, from the urea group to the naphthyl moiety. Comparing compounds that do not form hydrogen bond with acetate, the spatial distribution of the HOMO in ***m*-2urea** is mostly localised on the phenyl-group substituents of the naphthalene ring system, and the LUMO orbitals are distributed on the naphthyl rings; the molecular orbitals are not distributed over the urea group (Supplementary Fig. 12). However, in ***p*-2urea**, the HOMO and LUMO molecular orbitals are distributed around the naphthalene ring system, and it can be seen that the LUMO molecular orbitals are distributed in the urea group. Thus, ***p*-2urea** can be assumed to have greater overlap between its HOMO and LUMO orbitals than ***m*-2urea**, having greater oscillator strength on the long wavelength side of the UV–Vis spectrum (Supplementary Fig. 13 and Supplementary Table 4).

Compared with the molecular orbitals of the hydrogen-bonded acetate complexes, the same tendency is seen for ***m*-2urea**, and the molecular orbitals in the hydrogen-bonded complex of ***m*-2urea** with acetate are strongly localised to specific substituents (Supplementary Fig. 14). For the HOMO of the hydrogen-bonded complex of ***m*-2urea**, no electron density was observed on the naphthalene ring, which suggests

that there is weaker absorption in the long wavelength region for this complex because there is little overlap between the HOMO and LUMO orbitals (Supplementary Fig. 15 and Supplementary Table 5). These calculation results are in agreement with the difference in the shape of the experimental absorption spectra for the two positional isomers on the long-wavelength side.

The emission spectrum of ***p*-2urea** in DMSO (150 μM) is characterised by an unstructured broad band centred at 436 nm (λ_{ex} = 359 nm), while the emission maxima of ***p*-1urea** and ***m*-2urea** in DMSO (150 μM) occur at 399 and 423 nm, respectively. These results indicate that the extent of the π-conjugation in ***p*-2urea** is greater than those in ***p*-1urea** and ***m*-2urea**. The addition of TBAAc (up to 250 equiv) induced a substantial quenching of the ***p*-2urea** emission,[30] while a new emission band developed at lower energies (Fig. 3). It was suggested that the lower-energy band originates from a charge-transfer transition involving a tautomeric form of the FL urea–acetate IHBC in which the N–H proton of the urea groups is transferred from urea to acetate in the excited state[38]. Upon the addition of a large excess of acetate (>250 equiv), a new emission band developed at 450 nm, the intensity of which did not reach a limiting value even at 20000 equiv. It is worth mentioning that the intensity value of the new emission band at 20000 equiv is higher than that of the ***p*-2urea** emission band before the addition of TBAAc. Changes in the emission spectra of ***p*-1urea** and ***m*-2urea** upon adding excess TBAAc were also investigated, to examine the generality and characteristics of the nonlinear fluorescence intensity change phenomenon. The nonlinear phenomenon was also observed for ***p*-1urea** and ***m*-2urea**, although the fluorescence intensity increase for ***p*-1urea** was minimal, and the value for ***m*-2urea** was even smaller compared to that of ***p*-2urea** (Figs. 3 and S17). These experimental results indicate that the nonlinear phenomenon upon adding of TBAAc is a general phenomenon for fluorescent urea compounds with a phenylnaphthalene skeleton, and π-conjugation from the hydrogen-bonded urea groups to the naphthyl groups is probably an important factor because of the significant difference between the results for ***p*-2urea** and ***m*-2urea**.

Thus, we concluded that the nonlinear phenomenon caused by the addition of acetate was a result of the ionic hydrogen bonds between acetate ions and urea groups, which increased the electron-donor character of the urea group and caused intramolecular charge-transfer fluorescence and TICT fluorescence. In general, fluorophores exhibiting TICT fluorescence often display fluorescence intensity increases with increasing solvent viscosity and aggregation-induced emission enhancement[23]. In addition, solutions with an excess of TBAAc are considered to exhibit high viscosity because the acetate anion and tetrabutylammonium cation of TBAAc experience a Coulomb force[39]. Therefore, we investigated the relationship between the increase in fluorescence intensity and the solvent viscosity change when adding an excess of TBAAc.

Viscosity dependence of fluorescence intensity

First, viscosity increases occurring upon adding TBAAc to DMSO were measured using a viscometer, revealing that the solvent viscosity was increased from 2.3 to 4.7 cP as the amount TBAAc was increased from 250 to 20000 equiv. The Förster–Hoffmann equation[40, 41] describes the relationship between the fluorescence quantum yield and viscosity. To understand this relationship in our system, we plotted the ratio of the FL intensities at 452 nm of ***p*-2urea** before and after the addition of ≥250 equiv of TBAAc (I/I_{250eq}) versus viscosity (Fig. 4). A linear relationship with a slope of 3.7 (R^2 = 0.999) was obtained in the viscosity range from 2.3 to 4.7 cP at 25 °C, as expressed by the following equation (Eq. 1):

$$\log(I/I_{250eq}) = C + x\log(\eta\ /\mathrm{cP}), \qquad (1)$$

where η is the viscosity and C is a proportionality constant that depends on concentration and temperature. The slope x is the most important parameter for evaluating the viscosity-sensing capabilities of probe materials because the value is probe-dependent and reflects the degree of change in I with respect to η. Values of x = 3.7 and C = −1.4 were determined for this molecular system. The torsional motions of the phenyl ring substituents of naphthalene should be inhibited as the viscosity of the media increases. Thus, nonradiative emission decay caused by this motion the phenyl rings should be effectively suppressed in more viscous media. It should be noted that x = 3.7 for the probe-dependent constant is a remarkably high value, compared, for example, with x = 0.59 for 9-(dicyanovinyl)julolidine (DCVJ) in a mixture of glycerol and ethylene glycol, a well-known highly viscosity-sensitive fluorescent probe[23, 42].

Next, to examine the effects of ionic hydrogen bonding between urea groups and acetate anions on viscosity sensitivity, FL measurements of ***p*-2urea** in a mixture of glycerol and DMSO, without adding TBAAc, were performed as a control experiment. The relationship between the fluorescence intensity at 436 nm and viscosity was examined with a fixed concentration of ***p*-2urea** (1.5 μM) in mixed DMSO–glycerol solvents of various DMSO: glycerol ratios to modulate viscosity [DMSO/glycerol (v/v) = 10/0, 9/1, 8/2, 7/3, 6/4, 5/5, 4/6, 3/7, 2/8, and 1/9] (Supplementary Fig. 18). For the mixed solvents with glycerol amounts up to 80%, the emission intensity at an excitation wavelength of 359 nm increased with viscosity. Indeed, the emission intensity of ***p*-2urea** in 80% glycerol was significantly increased, being 1.7-fold greater than that without glycerol. However, in the solvent with a 90% glycerol content, the FL intensity decreased with increasing concentration because of the aggregation of ***p*-2urea**, which is insoluble in glycerol. The sensitivity constant of the dye, x in equation (1), was found to be 0.12 (R^2 = 0.971). Therefore, ***p*-2urea** without ionic hydrogen bonding with acetate displayed low viscosity sensitivity. The viscosity sensitivities of IHBCs of ***m*-2urea** and ***p*-1urea** with acetate ions were also investigated in the presence of excess amounts of TBAAc, and lower viscosity sensitivities than that of ***p*-2urea** were obtained (Supplementary Figs. S19 and S20). These results indicate that the FL intensity of the ***p*-2urea**–acetate ion IHBC strongly depends on fluid viscosity.

Changes in fluorescence properties in solution and the solid state due to the addition of acetate ions

The absolute fluorescence quantum yields (QYs) in solution, in the absence and presence of TBAAc, were measured to confirm whether ***p*-2urea** shows AIEE in the presence of TBAAc. Measurement of FL QYs in the solid-state involves using a powder containing microcrystals obtained by slowly distilling off the solvent and an amorphous state after being ground in a mortar for 10 min, because FL QYs often change depending on the morphology of the FL material, i.e., whether it is in a microcrystalline or amorphous state.

The fluorescence QY of DMSO solution of ***p*-2urea** was 18%, while the QYs of powdered ***p*-2urea**, which contained microcrystalline and amorphous material, were 7% and 25% before and after grinding, respectively (Fig. 5). These unexpected differences between powders before and after grinding may be useful for mechano-stimuli-responsive luminescent materials. The FL QYs of the IHBC of ***p*-2urea** and acetate were also measured, in solution and in the solid state. The FL QY of the IHBC DMSO solution to which 200 equiv of TBAAc had been added, in which the ionic hydrogen bonding between urea groups and acetate ions is considered to be saturated, was revealed to be 7%. However, the solid-state ***p*-2urea**–acetate IHBC, prepared by drop casting the solution of ***p*-2urea** with 5 equiv of TBAAc, produced a QY of 41%, which is more than five times higher than that of the solution-phase IHBC. These results indicate that IHBC exhibits AIEE. The IHBC of ***p*-2urea** and acetate ions in the solid-state with 5 equiv of TBAAc exhibits an emission red-shift of approximately 18 nm relative to the emission of ***p*-2urea** powder in the absence of TBAAc (Fig. 6). In addition, the effects of the amount of TBAAc on the QY of the mixture of ***p*-2urea** and TBAAc were investigated by adding 2, 5, 10, 30, 60, 100, and 1800 equiv of TBAAc to the solid-state sample, resulting in FL QYs of 37, 41, 39, 31, 29, 29, and 29%, respectively (Supplementary Fig. 21). These results indicate that the cause of the increase in QY of the IHBC in the solid-state was neither the suppression of intermolecular interactions of the IHBC nor the suppression of self-absorption in the presence of an excess of TBAAc. Furthermore, the effects of the addition of TBAAc to ***p*-1urea** and ***m*-2urea** were also investigated. In the case of ***m*-2urea**, the QY of the DMSO solution was 17% (Supplementary Fig. 22). However, the powder containing microcrystals and the powder after grinding exhibited QYs of 37 and 34%, respectively. Interestingly, ***m*-2urea** shows AIEE even without adding TBAAc, which is an opposite result to that of ***p*-2urea**. In addition, the DMSO solution of IHBC exhibited 2% QY and the complex with 5 equiv of TBAAc in the solid-state exhibited a QY of 18%. The emission of the ***m*-2urea**–acetate ion IHBC in the solid state is red-shifted by 21 nm relative to the ***m*-2urea** powder emission in the absence of TBAAc (Supplementary Fig. 23).

In the case of ***p*-1urea**, the DMSO solution without TBAAc shows a high QY of 54%, while the QYs of the powder including microcrystals and the powder after grinding are 44 and 47%, respectively (Supplementary Fig. 24). In addition, the QY of the IHBC of ***p*-1urea** and acetate ions was 3% in solution and the QY of the IHBC increased to 50% in the solid-state in the presence of 5 equiv of TBAAc. The ***p*-1urea**–acetate ion IHBC in the solid-state exhibits an emission red-shift of approximately 9 nm relative to ***p*-1urea** powder in the absence of TBAAc (Supplementary Fig. 25).

These results indicate that IHBC of ***p*-2urea**, ***p*-1urea**, and ***m*-2urea** with acetate ions exhibit much higher QYs in the solid state than in solution. In particular, the IHBC of ***p*-2urea** and ***p*-1urea** with acetate ions in the solid-state exhibit higher QYs than those in the absence of TBAAc in the solid-state. In addition, the tendency of the IHBC QY to increase in the solid-state corresponds to enhanced fluid viscosity sensitivity for the fluorescence intensity.

Conclusions

In summary, we focused on urea groups, which are known to significantly change electron-donating properties by forming strong ionic hydrogen bonds with anion molecules, and investigated the optical properties of neutral fluorescent molecules and IHBCs of fluorescent urea derivatives and acetate ions in both solid-state and solution phases. These results revealed that IHBCs exhibited AIEE and remarkably high sensitivity to fluid viscosity. These interesting phenomena show the potential for the control of the characteristics of luminescent dyes by harnessing ionic hydrogen bonding interactions with molecular anions and highlight a new approach for the development of solid-state light-emitting materials and viscosity probes. This approach has infinite possibilities since there is an abundance of molecular anions with various structures and functions. A comprehensive investigation on superior urea architectures and molecular anions are currently in progress.

References

1. Thomas, S. W., 3rd et al. Chemical sensors based on amplifying fluorescent conjugated polymers. *Chem Rev.* **107**, 1339-1386 (2007).
2. Luo, J. et al. Aggregation-induced emission of 1-methyl-1,2,3,4,5-pentaphenylsilole. *Chem Commun.* 1740-1741 (2001).
3. Mei, J. et al. Aggregation-induced emission: together we shine, united we soar! *Chem Rev.* **115**, 11718-11940 (2015).
4. Luo, Y. et al. Facile Access to Twisted Intramolecular Charge-Transfer Fluorogens Bearing Highly Pretwisted Donor–Acceptor Systems Together with Readily Fine-Tuned Charge-Transfer Characters. *Small.* **13**, 1604113 (2017).
5. Zhou, H. et al. Aggregation-induced emission (AIE)-active polymers for explosive detection. *Polymer Chemistry.* **10**, 3822-3840 (2019).
6. Qiu, J. et al. A fluorescent sensor based on aggregation-induced emission: highly sensitive detection of hydrazine and its application in living cell imaging. *Analyst.* **143**, 4298-4305 (2018).
7. Jin, Y.-J. et al. Molecular rotors with long alkyl chains as fluorescent viscosity sensors for hydrocarbon and silicone oil fluids. *J Mol Liq.* **276**, 1-6 (2019).
8. Qian, J. et al. AIE luminogens for bioimaging and theranostics: from organelles to animals. *Chem.* **3**, 56-91 (2017).

9. Iida, A. et al. Intense solid-state blue emission with a small Stokes' shift: π-stacking protection of the diphenylanthracene skeleton. *Chemical Communications.* 3002-3004 (2009).
10. An, B.-K. et al. Enhanced emission and its switching in fluorescent organic nanoparticles. *J Am Chem Soc.* **124**, 14410-14415 (2002).
11. Wang, Y. et al. Aqueous nanoaggregation-enhanced one-and two-photon fluorescence, crystalline J-aggregation-induced red shift, and amplified spontaneous emission of 9, 10-bis (p-dimethylaminostyryl) anthracene. *The Journal of Physical Chemistry C.* **116**, 15576-15583 (2012).
12. Sasaki, S. et al. Aggregation-induced emission active D-π-A binaphthyl luminophore with dual-mode fluorescence. *RSC advances.* **4**, 33474-33477 (2014).
13. Sasaki, S. et al. Highly twisted N, N-dialkylamines as a design strategy to tune simple aromatic hydrocarbons as steric environment-sensitive fluorophores. *J Am Chem Soc.* **138**, 8194-8206 (2016).
14. Caruso, U. et al. AIE/ACQ effects in two DR/NIR emitters: A structural and DFT comparative analysis. *Molecules.* **23**, 1947 (2018).
15. Mutai, T. et al. Switching of polymorph-dependent ESIPT luminescence of an imidazo [1, 2-a] pyridine derivative. *Angewandte Chemie International Edition.* **47**, 9522-9524 (2008).
16. Kono, L. et al. Aggregation-induced emission effect on turn-off fluorescent switching of a photochromic diarylethene. *Beilstein J Org Chem.* **15**, 2204-2212 (2019).
17. Dong, Y. et al. Aggregation-induced emissions of tetraphenylethene derivatives and their utilities as chemical vapor sensors and in organic light-emitting diodes. *Applied physics letters.* **91**, 011111 (2007).
18. Hansmann, M. M. et al. B (C6F5) 3: a Lewis acid that brings the light to the solid state. *Angewandte Chemie International Edition.* **55**, 1196-1199 (2016).
19. Ren, Y. et al. Multistimuli-responsive enaminitrile molecular switches displaying H+-induced aggregate emission, metal ion-induced turn-on fluorescence, and organogelation properties. *J Am Chem Soc.* **140**, 13640-13643 (2018).
20. Benson, C. R. et al. Plug-and-play optical materials from fluorescent dyes and macrocycles. *Chem.* **6**, 1978-1997 (2020).
21. Wang, J. et al. Ionization and anion− π+ interaction: a new strategy for structural design of aggregation-induced emission luminogens. *J Am Chem Soc.* **139**, 16974-16979 (2017).
22. Hu, R. et al. Twisted intramolecular charge transfer and aggregation-induced emission of BODIPY derivatives. *The Journal of Physical Chemistry C.* **113**, 15845-15853 (2009).
23. Haidekker, M. A. et al. Molecular rotors—fluorescent biosensors for viscosity and flow. *Org Biomol Chem.* **5**, 1669-1678 (2007).
24. Liu, D. et al. A novel approach towards white photoluminescence and electroluminescence by controlled protonation of a blue fluorophore. *Chemical Communications.* **49**, 10001-10003 (2013).
25. Xiong, J. et al. Multi-stimuli-responsive fluorescence switching from a pyridine-functionalized tetraphenylethene AIEgen. *ACS applied materials & interfaces.* **10**, 5819-5827 (2018).

26. Lee, J. Y. et al. Efficient fluoride-selective fluorescent host: Experiment and theory. *The Journal of organic chemistry.* **69**, 943-950 (2004).
27. Amendola, V. et al. Anion recognition by hydrogen bonding: urea-based receptors. *Chem Soc Rev.* **39**, 3889-3915 (2010).
28. Zhou, Y. et al. Fluorescence and colorimetric chemosensors for fluoride-ion detection. *Chem Rev.* **114**, 5511-5571 (2014).
29. Busschaert, N. et al. Applications of Supramolecular Anion Recognition. *Chem Rev.* **115**, 8038-8155 (2015).
30. Amendola, V. et al. The interaction of fluoride with fluorogenic ureas: an ON1–OFF–ON2 response. *J Am Chem Soc.* **135**, 6345-6355 (2013).
31. Duke, R. M. et al. 3-Urea-1, 8-naphthalimides are good chemosensors: a highly selective dual colorimetric and fluorescent ICT based anion sensor for fluoride. *Tetrahedron Lett.* **52**, 1503-1505 (2011).
32. Takahashi, M. et al. A novel approach to white-light emission using a single fluorescent urea derivative and fluoride. *New Journal of Chemistry.* **43**, 3265-3268 (2019).
33. Lee, C. et al. Development of the Colle-Salvetti correlation-energy formula into a functional of the electron density. *Physical review B.* **37**, 785 (1988).
34. Yanai, T. et al. A new hybrid exchange–correlation functional using the Coulomb-attenuating method (CAM-B3LYP). *Chem Phys Lett.* **393**, 51-57 (2004).
35. Frisch, M. J. et al. Gaussian 16 Rev. C.01. Wallingford, CT; 2016.
36. Bregović, V. B. et al. Anion binding with urea and thiourea derivatives. *Coord Chem Rev.* **295**, 80-124 (2015).
37. Banerji, B. et al. Molecular details of acetate binding to a new diamine receptor by NMR and FT-IR analyses. *The Journal of Physical Chemistry A.* **120**, 2330-2341 (2016).
38. Matsumoto, H. et al. Kinetic analysis of tautomer forms of aromatic-urea compounds with acetate ions: solvent effect of excited state intermolecular proton transfer. *Photochemical & Photobiological Sciences.* **17**, 561-569 (2018).
39. Paduszyński, K. et al. Viscosity of ionic liquids: an extensive database and a new group contribution model based on a feed-forward artificial neural network. *J Chem Inf Model.* **54**, 1311-1324 (2014).
40. Bhagwat, A. A. et al. Viscosity-active D-π-A chromophores derived from benzo [b] thiophen-3 (2H)-one 1, 1-dioxide (BTD): Synthesis, photophysical, and NLO properties. *Spectrochimica Acta Part A: Molecular and Biomolecular Spectroscopy.* **203**, 244-257 (2018).
41. Lee, W.-E. et al. Fluorescent viscosity sensor film of molecular-scale porous polymer with intramolecular π-stack structure. *Macromolecules.* **44**, 432-436 (2011).
42. Kotani, R. et al. Flapping viscosity probe that shows polarity-independent ratiometric fluorescence. *Journal of Materials Chemistry C.* **5**, 5248-5256 (2017).

Figures

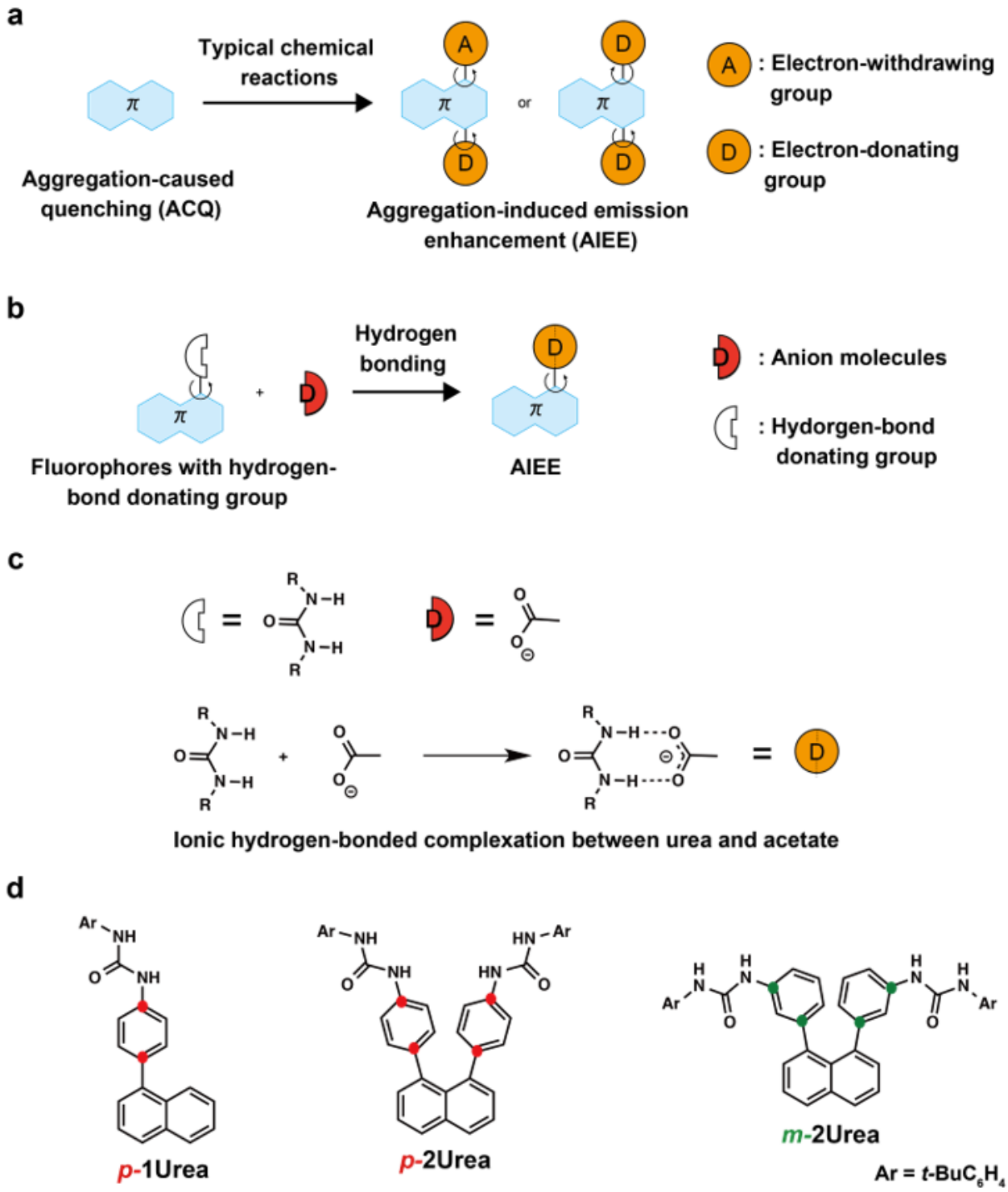

Figure 1

(a) Schematic illustration of the addition of electron-donating (D) and/or electron-withdrawing (A) groups to fluorophores to synthesise typical AIEE fluorophores. (b) Design strategy for ionic hydrogen-bonded complexes (IHBC) with viscosity-sensitive fluorescence and AIEE (this work). (c) Urea as hydrogen-bond

donating group and acetate as hydrogen-bond acceptor. (d) Chemical structures of model molecules: p-1urea, p-2urea, and m-2urea.

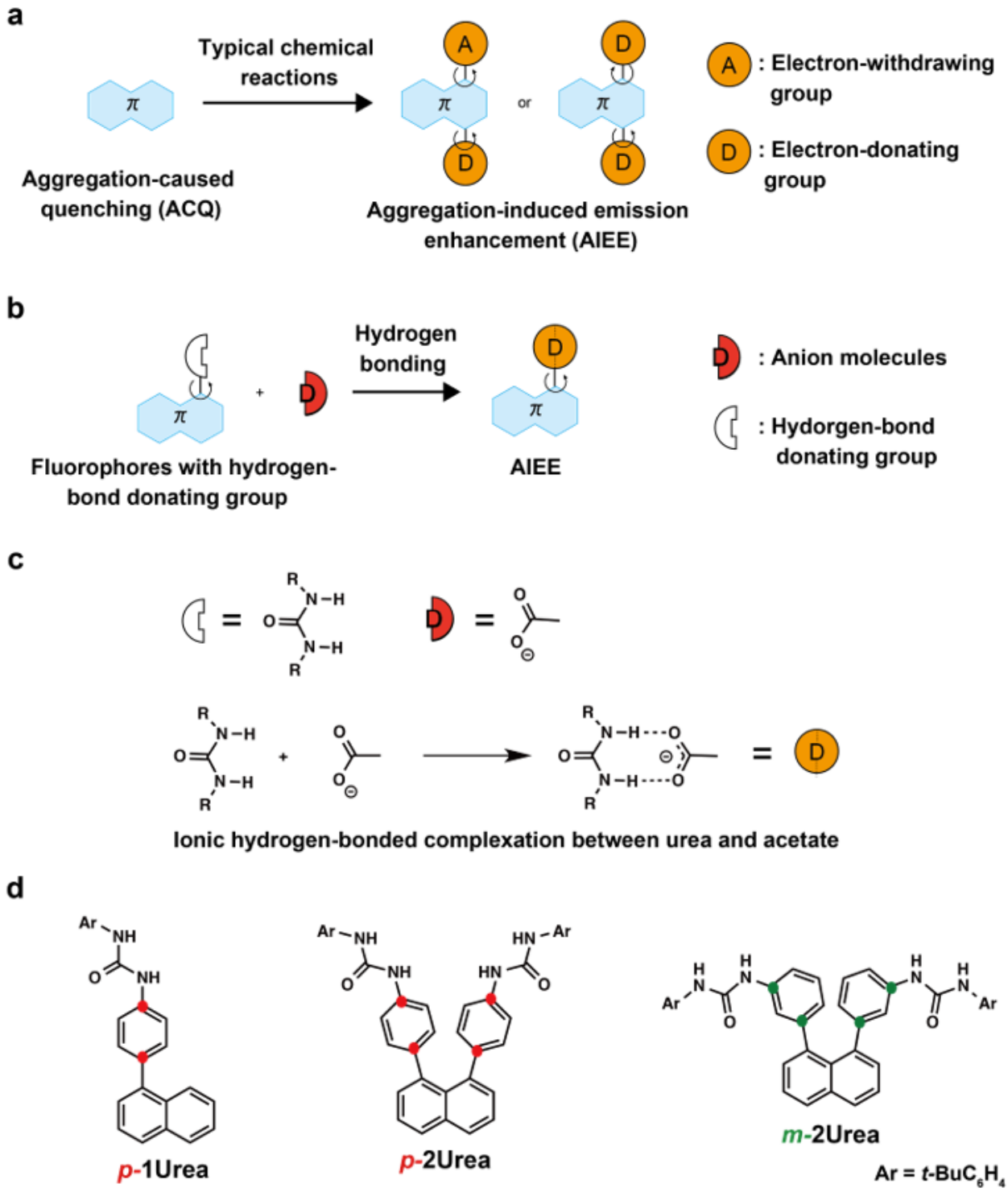

Figure 1

(a) Schematic illustration of the addition of electron-donating (D) and/or electron-withdrawing (A) groups to fluorophores to synthesise typical AIEE fluorophores. (b) Design strategy for ionic hydrogen-bonded complexes (IHBC) with viscosity-sensitive fluorescence and AIEE (this work). (c) Urea as hydrogen-bond

donating group and acetate as hydrogen-bond acceptor. (d) Chemical structures of model molecules: p-1urea, p-2urea, and m-2urea.

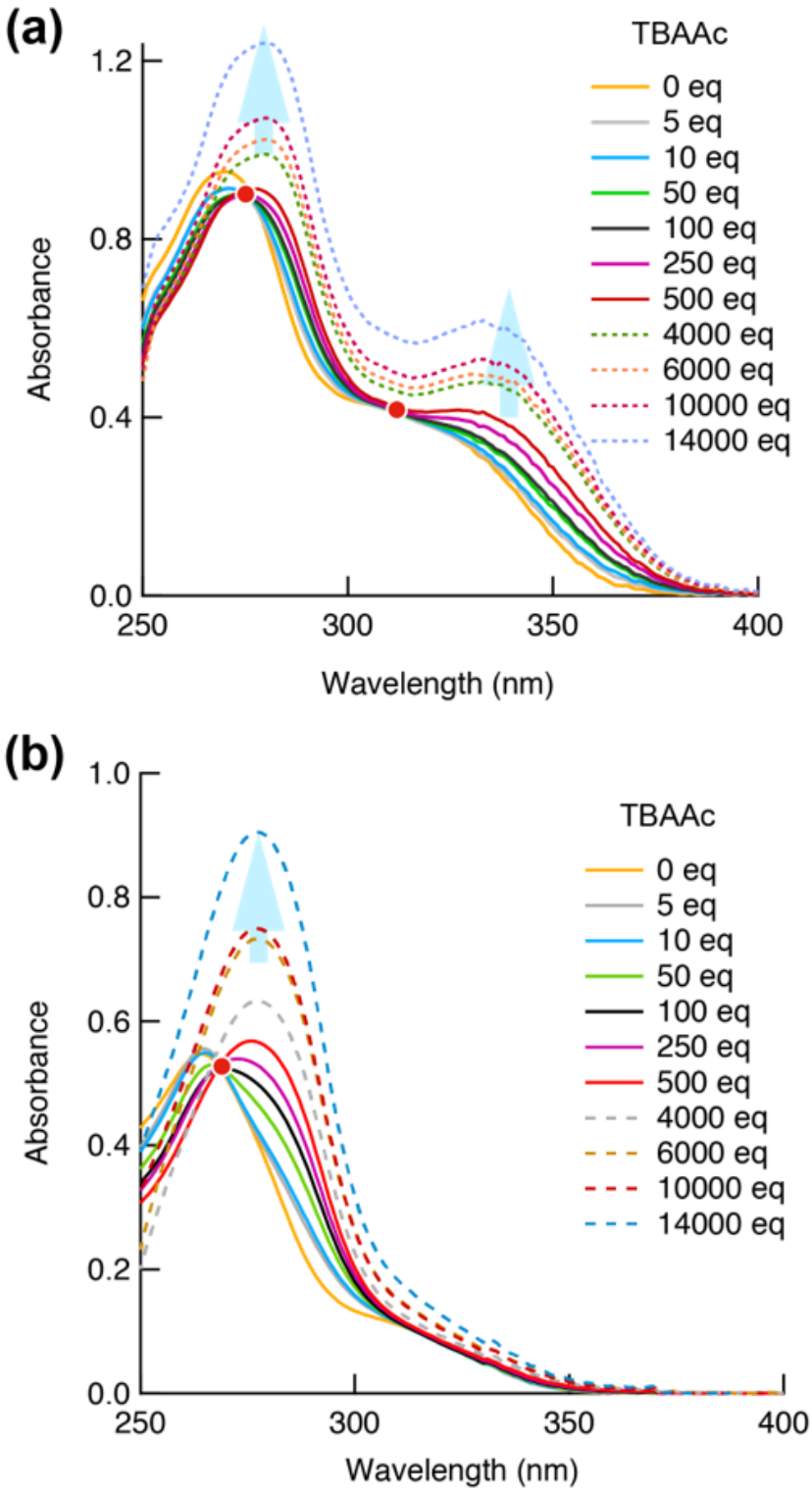

Figure 2

Absorbance spectra of (a) p-2urea and (b) m-2urea in the absence and presence of TBAAc.

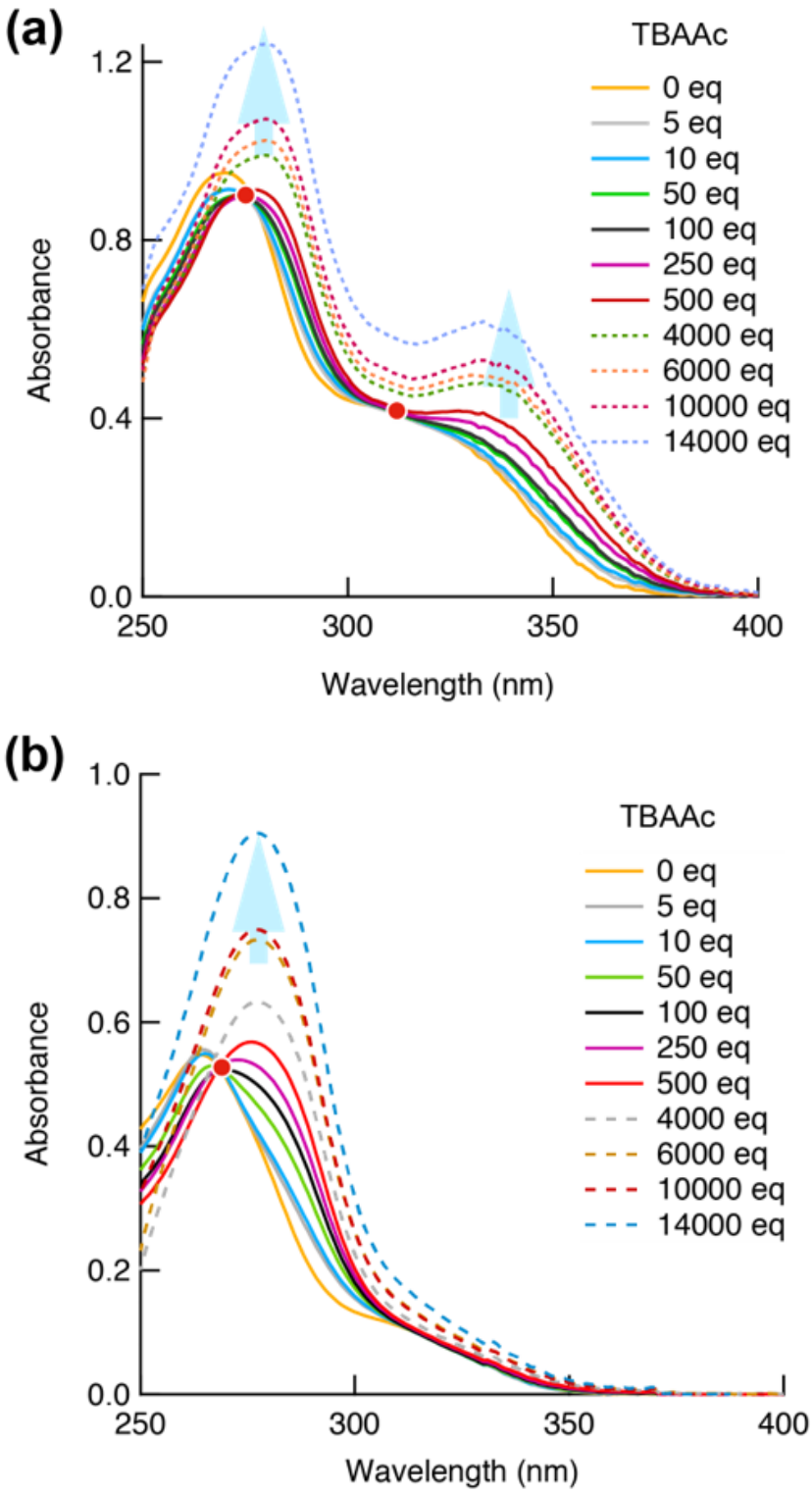

Figure 2

Absorbance spectra of (a) p-2urea and (b) m-2urea in the absence and presence of TBAAc.

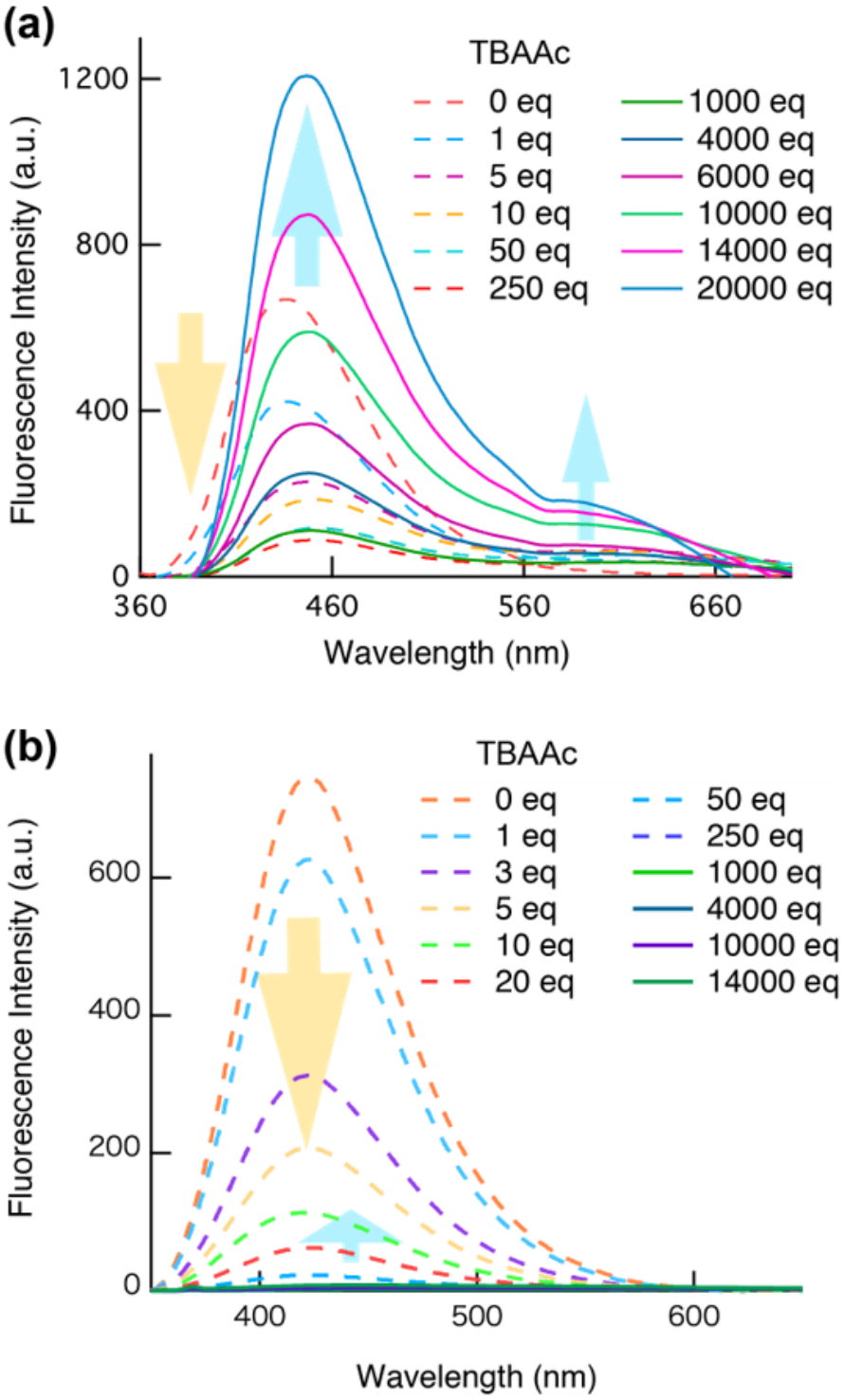

Figure 3

Fluorescence spectra of the urea derivatives in the absence and presence of different amounts of TBAAc. (a) Fluorescence spectra of a DMSO solution of p-2urea (150 μM, λex= 359 nm). (b) Fluorescence spectra of a DMSO solution of m-2urea (150 μM, λex = 332 nm).

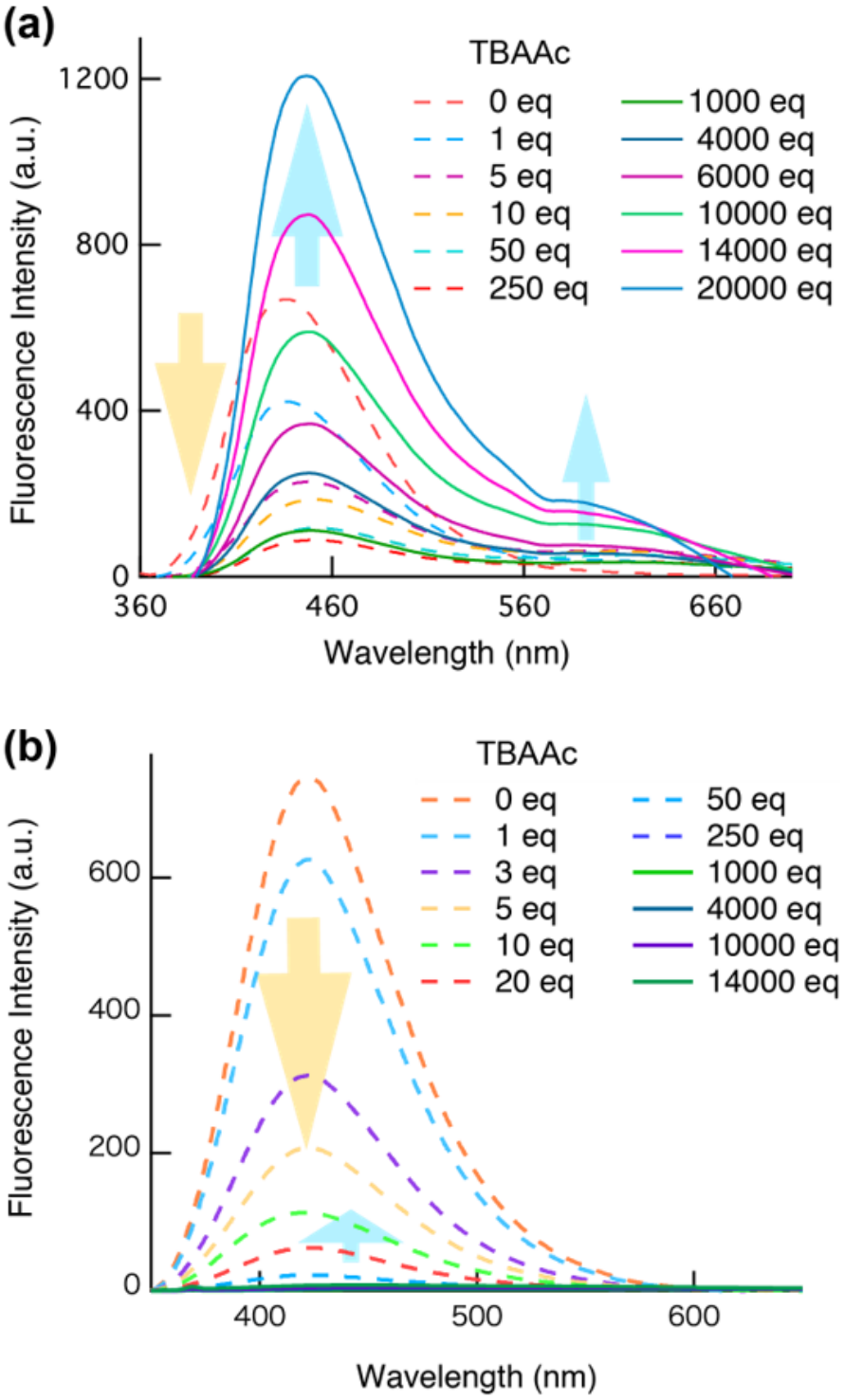

Figure 3

Fluorescence spectra of the urea derivatives in the absence and presence of different amounts of TBAAc. (a) Fluorescence spectra of a DMSO solution of p-2urea (150 μM, λex= 359 nm). (b) Fluorescence spectra of a DMSO solution of m-2urea (150 μM, λex = 332 nm).

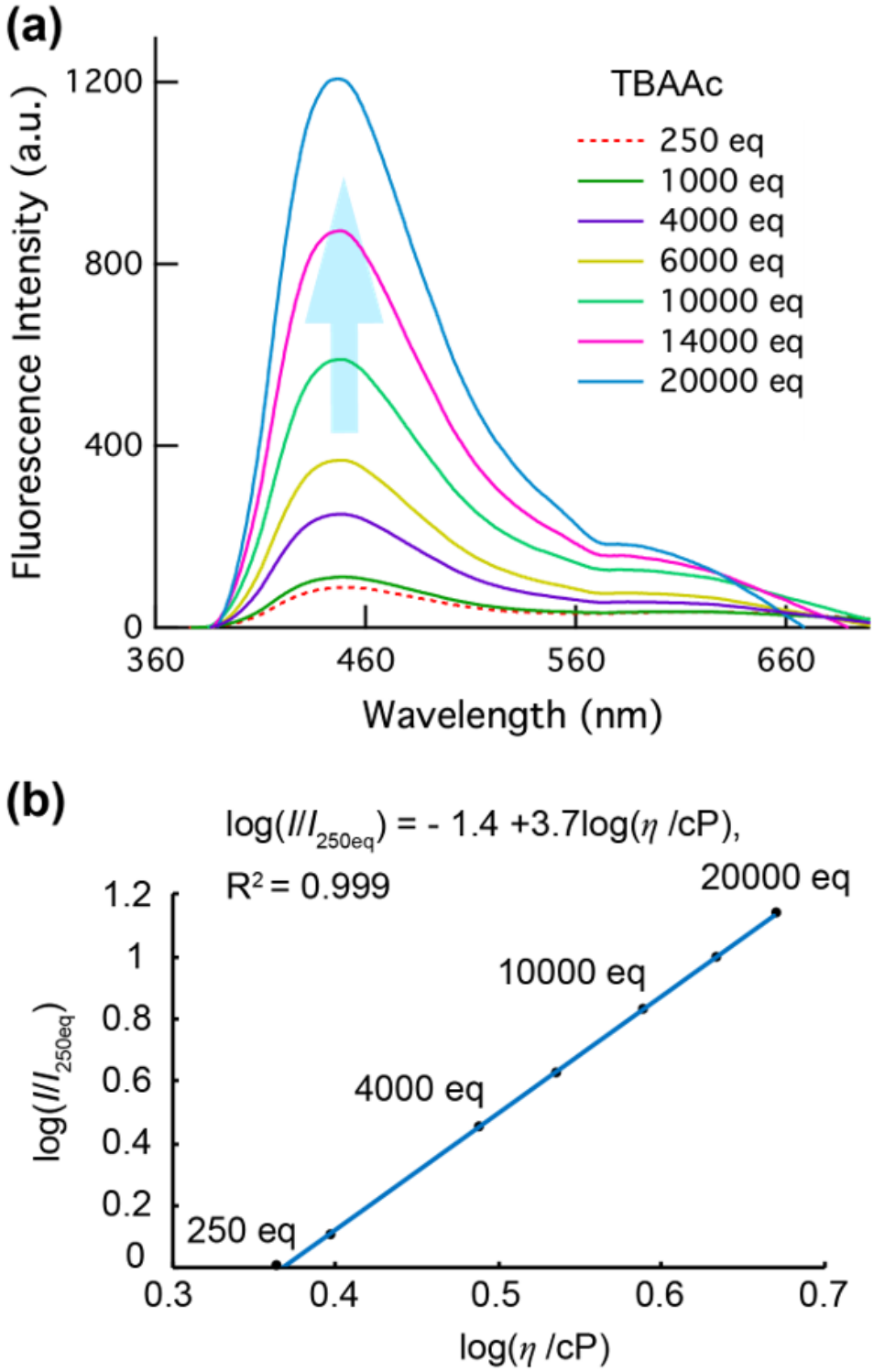

Figure 4

(a) Fluorescence spectra of p-2urea (150 μM, λex = 359 nm) with various excess amounts of TBAAc in DMSO. (b) Log–log plot of the ratio of fluorescence intensities before and after the addition of ≥250 equiv of TBAAc versus solvent viscosity.

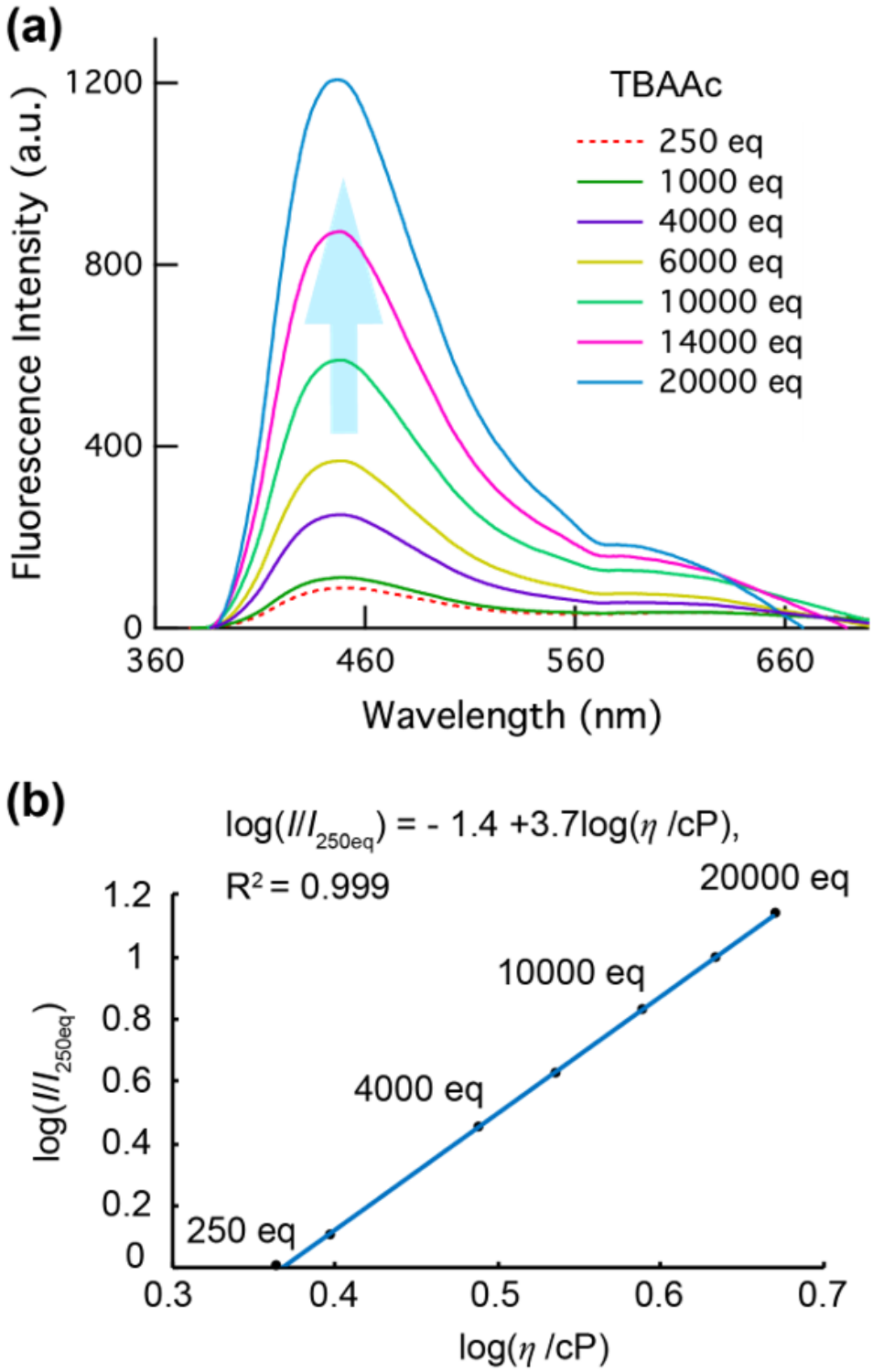

Figure 4

(a) Fluorescence spectra of p-2urea (150 μM, λex = 359 nm) with various excess amounts of TBAAc in DMSO. (b) Log–log plot of the ratio of fluorescence intensities before and after the addition of ≥250 equiv of TBAAc versus solvent viscosity.

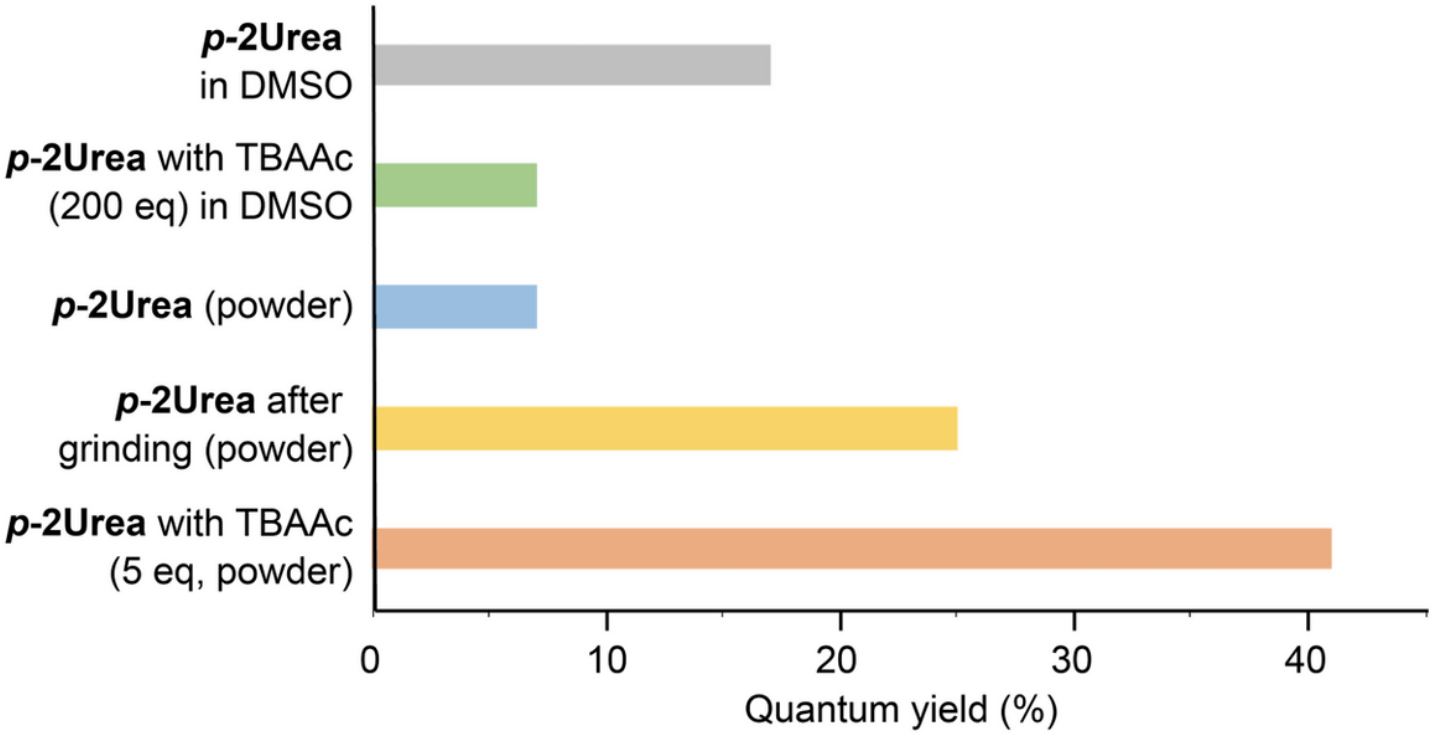

Figure 5

Absolute fluorescence quantum yields of p-2urea powder and p-2urea–DMSO solution in the absence and presence of TBAAc.

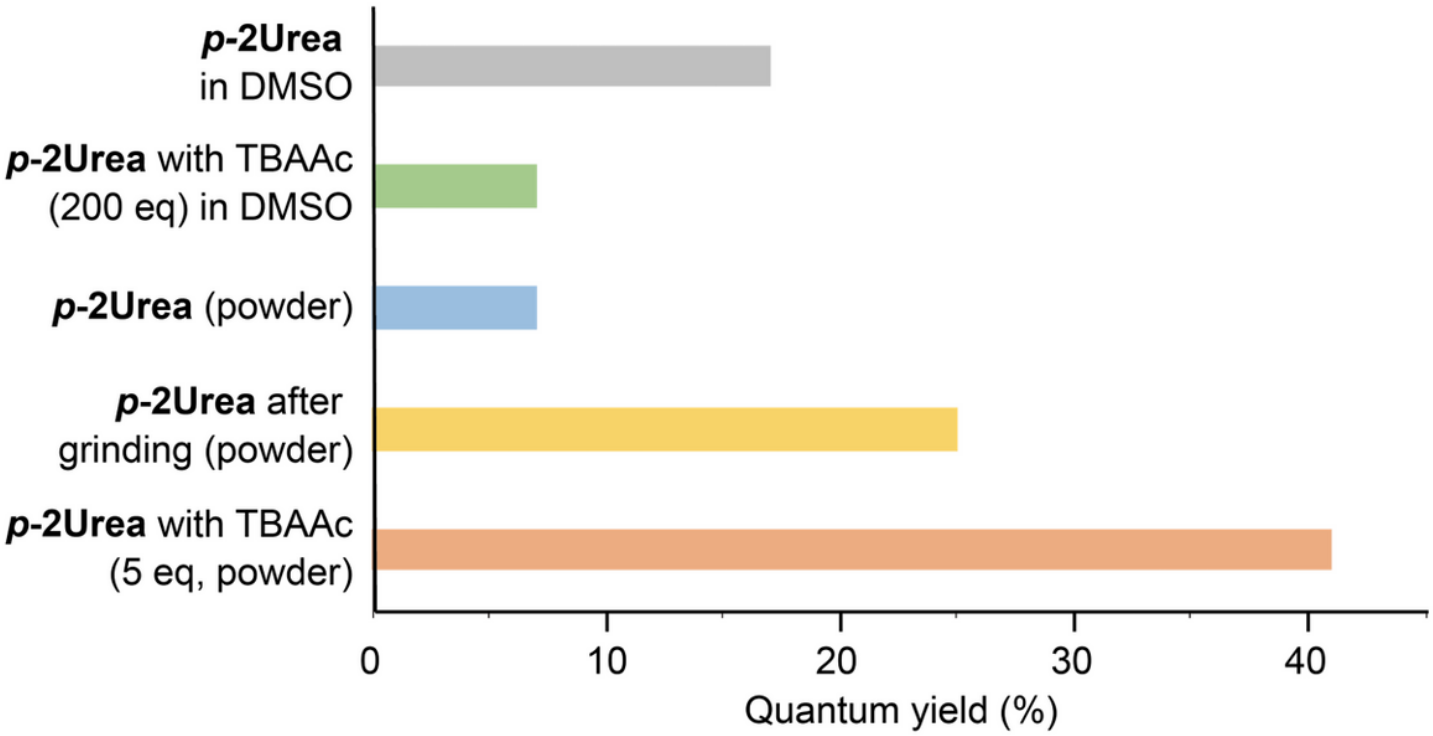

Figure 5

Absolute fluorescence quantum yields of p-2urea powder and p-2urea–DMSO solution in the absence and presence of TBAAc.

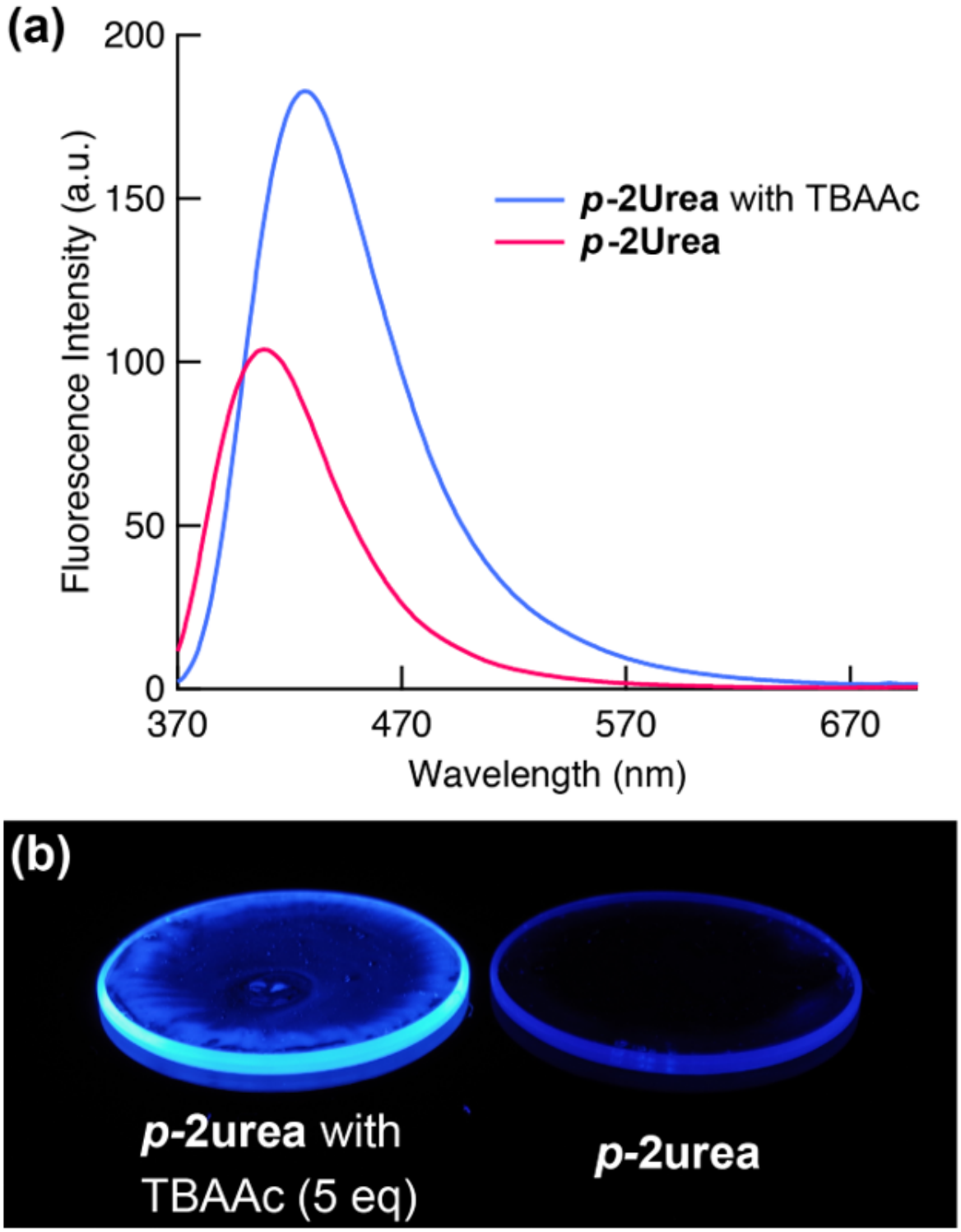

Figure 6

(a) Solid-state fluorescence spectra of p-2urea in the presence and absence of 5 equiv of TBAAc when excited at 340 nm. (b) Photographs of the same molar amount of p-2urea with 5 equiv of TBAAc (left)

and without TBAAc (right) on quartz plates prepared by drop casting under 365-nm ultraviolet-lamp irradiation.

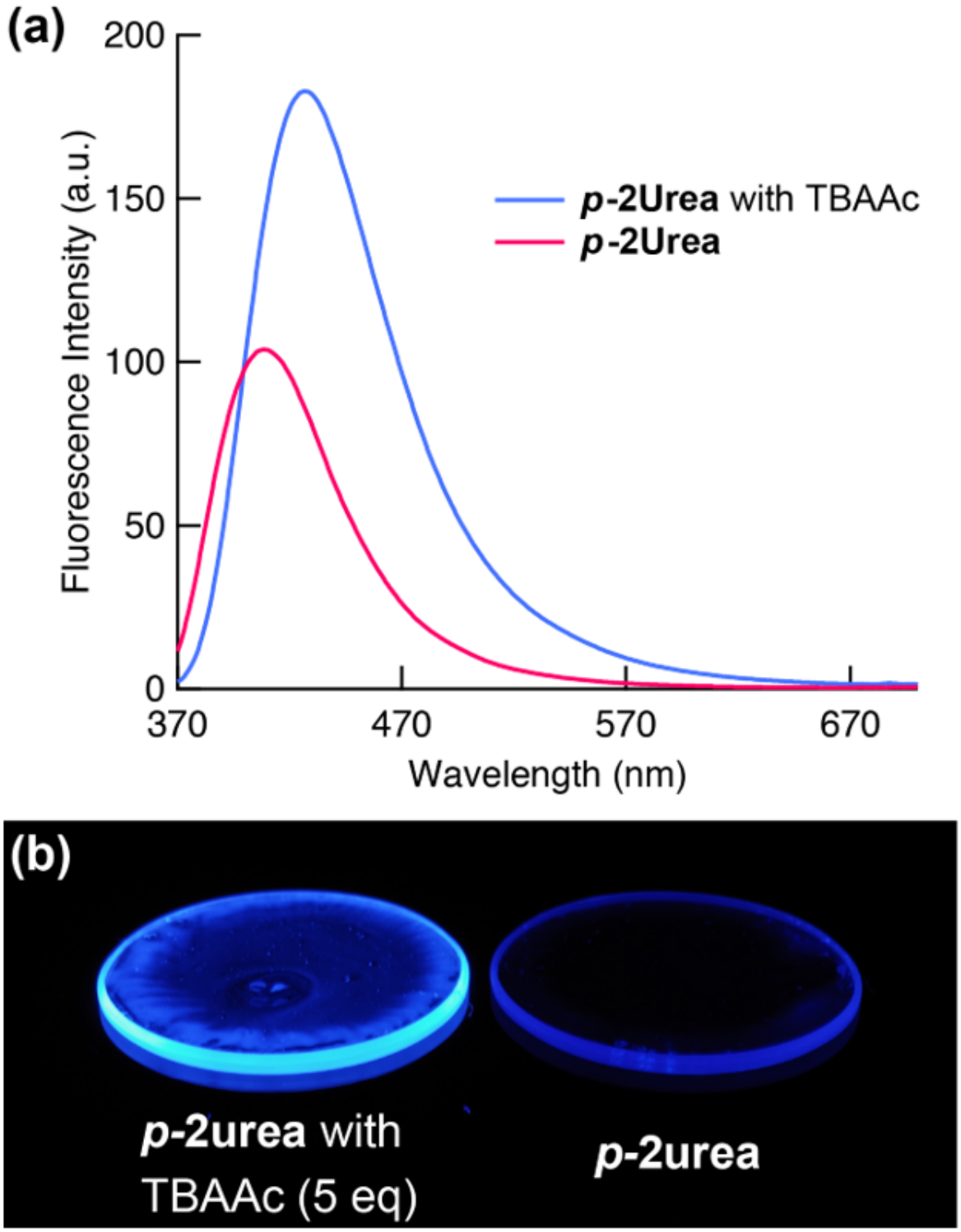

Figure 6

(a) Solid-state fluorescence spectra of p-2urea in the presence and absence of 5 equiv of TBAAc when excited at 340 nm. (b) Photographs of the same molar amount of p-2urea with 5 equiv of TBAAc (left)

and without TBAAc (right) on quartz plates prepared by drop casting under 365-nm ultraviolet-lamp irradiation.

Supplementary Files

This is a list of supplementary files associated with this preprint. Click to download.

- SupplementaryInformation.docx
- SupplementaryInformation.docx
- p2ureaa.cif
- p2ureaa.cif